

Figure 1. Morphology of herpesviruses. The viral particle is made of a capsid containing the viral genome, an intermediate proteic layer named tegument and a viral envelope with glycoproteins. The capsid is made of 150 hexons (green) and 11 pentons (blue) plus the portal protein to form an isocahedral structure (T=16) with pentons at the tops of the structure. One of the 12 tops is a pore by which DNA is enclosed in the capsid. From http://viralzone.expasy.org/all_by_species/181.html

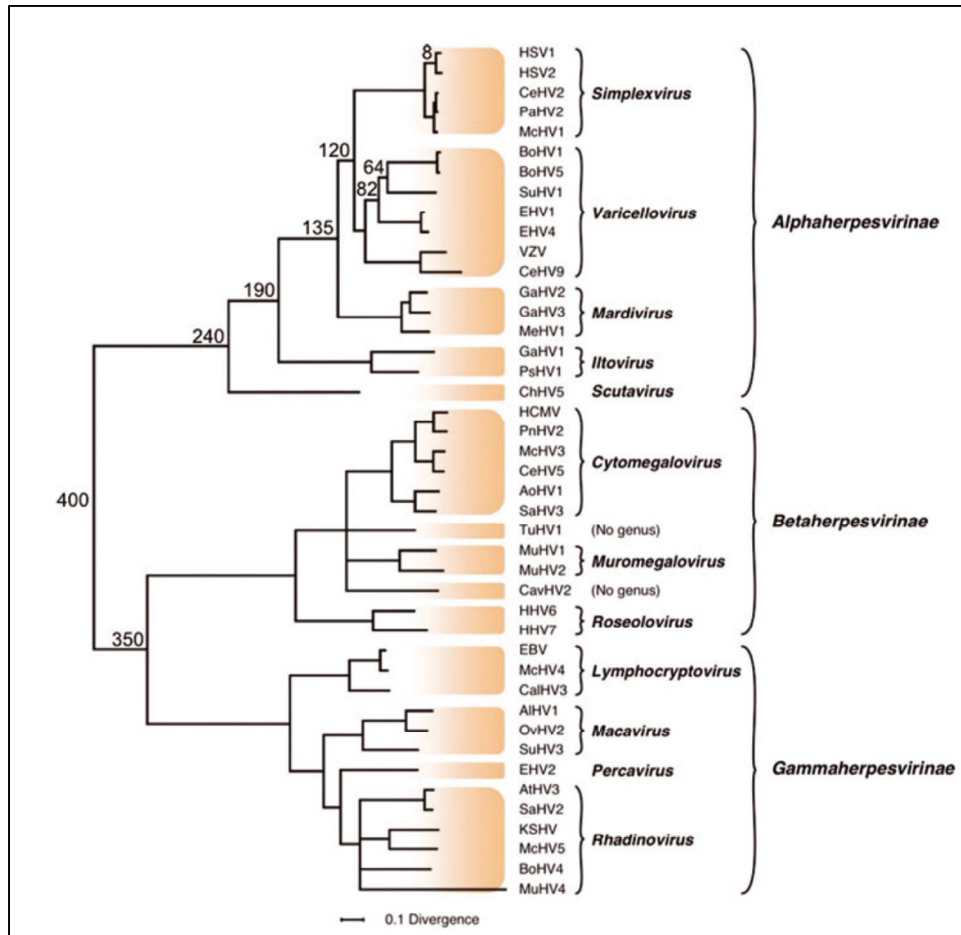


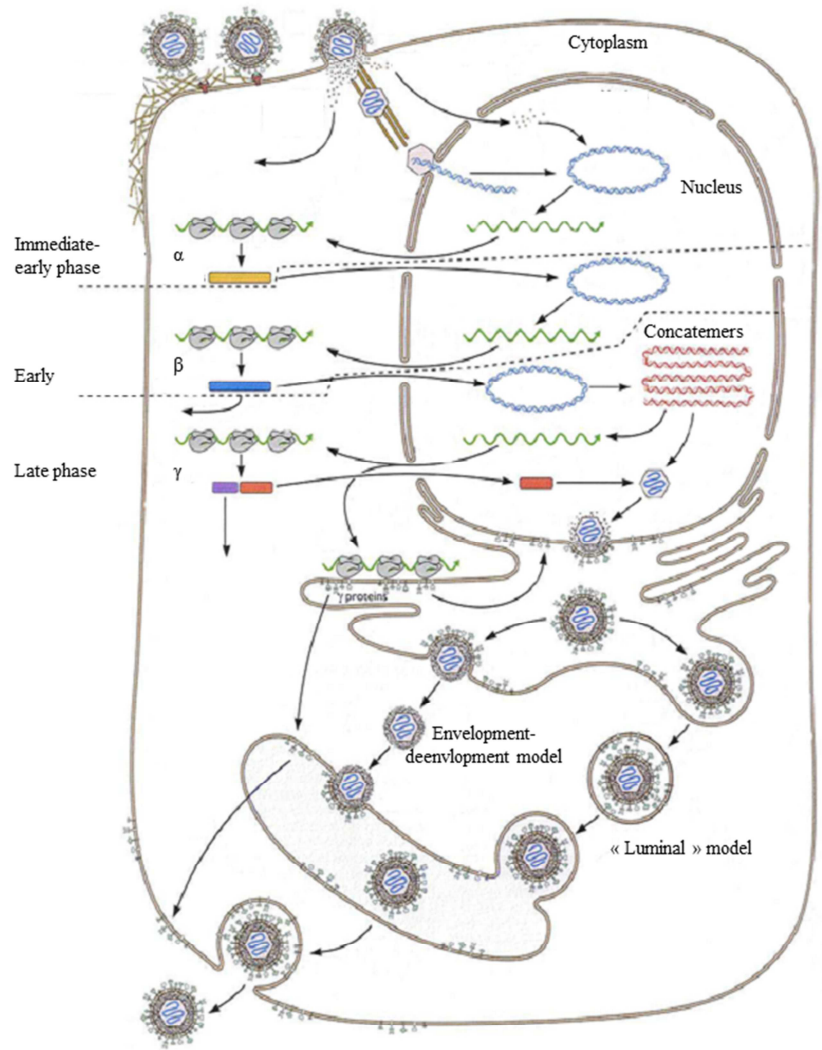
Figure 2. Classification of *Herpesviridae*. Phylogenetic tree for the family *Herpesviridae* adapted from Davison (2011). The Bayesian tree is based on amino acid sequence alignments for six genes (UL15, UL19, UL27, UL28, UL29, and UL30). The scale indicates substitutions per site. Approximate divergence dates (millions of years before present) are shown at selected nodes. The family *Herpesviridae* is composed of three subfamilies: the *alpha*-, *beta*- and *gamma*herpesvirinae and each one contains different genera.

A

Virus attachment to the cell surface and fusion with the plasma membrane

Viral proteins synthesis and viral DNA replication

Acquisition of viral membrane



B

Viral genome as a circular episomal element

Viral expression restricted to small amount of proteins

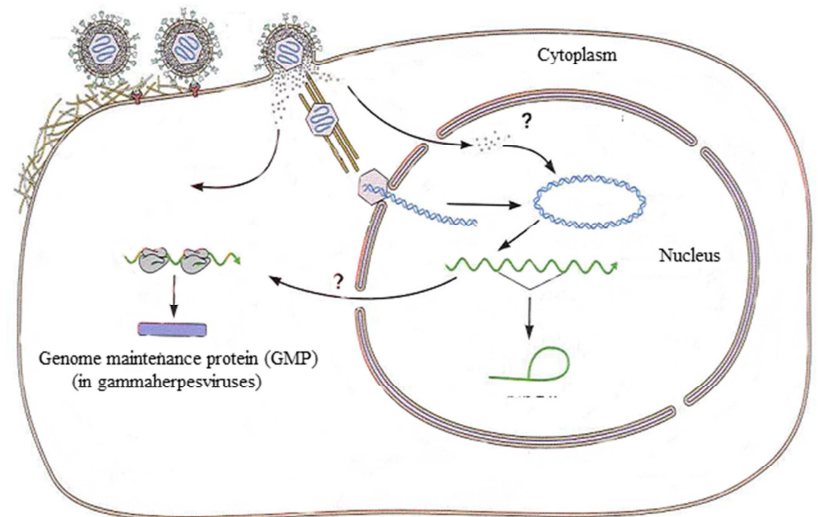


Figure 3. Representation of the general cycle of herpesviruses, including the lytic (A) and the latent (B) state. From Enquist *et al.* (2000).

Table I. Classification of the *gammaherpesvirinae*^a subfamily

Genera	Viral species	Abbreviation	Target cells	Natural Host/ Target host	Associated diseases
<i>Lymphocryptovirus</i>	Epstein-Barr virus or <i>human herpesvirus 4</i>	EBV or HHV-4	B Lymphocytes	Human	Infectious mononucleosis, Nasopharyngeal carcinoma Burkitt's lymphoma Hodgkin's lymphoma
<i>Rhadinovirus</i>	Kaposi sarcoma associated herpesvirus or <i>human herpesvirus 8</i>	KSHV or HHV-8	B Lymphocytes	Human	Kaposi sarcoma Castleman's disease Primary effusion lymphoma
	<i>Murid herpesvirus 4</i>	MuHV-4	B Lymphocytes / Macrophages	Small rodents	B cell lymphomas
	<i>Saimiriine herpesvirus 2</i>	SaHV-2	T Lymphocytes	Squirrel monkey/ other nonhuman primates	T cell lymphomas
<i>Percavirus</i>	<i>Equid herpesvirus 2</i>	EHV-2	B Lymphocytes	Horse	Respiratory diseases
<i>Macavirus</i>	<i>Ovine herpesvirus 2</i>	OvHV-2	T Lymphocytes	Sheep/ many ruminant species	Sheep-associated malignant catarrhal fever
	<i>Alcelaphine herpesvirus 1</i>	AiHV-1	T Lymphocytes	Wildebeest / many ruminant species	Wildebeest-derived malignant catarrhal fever

^aThe main members of the *gammaherpesvirinae* subfamily were selected

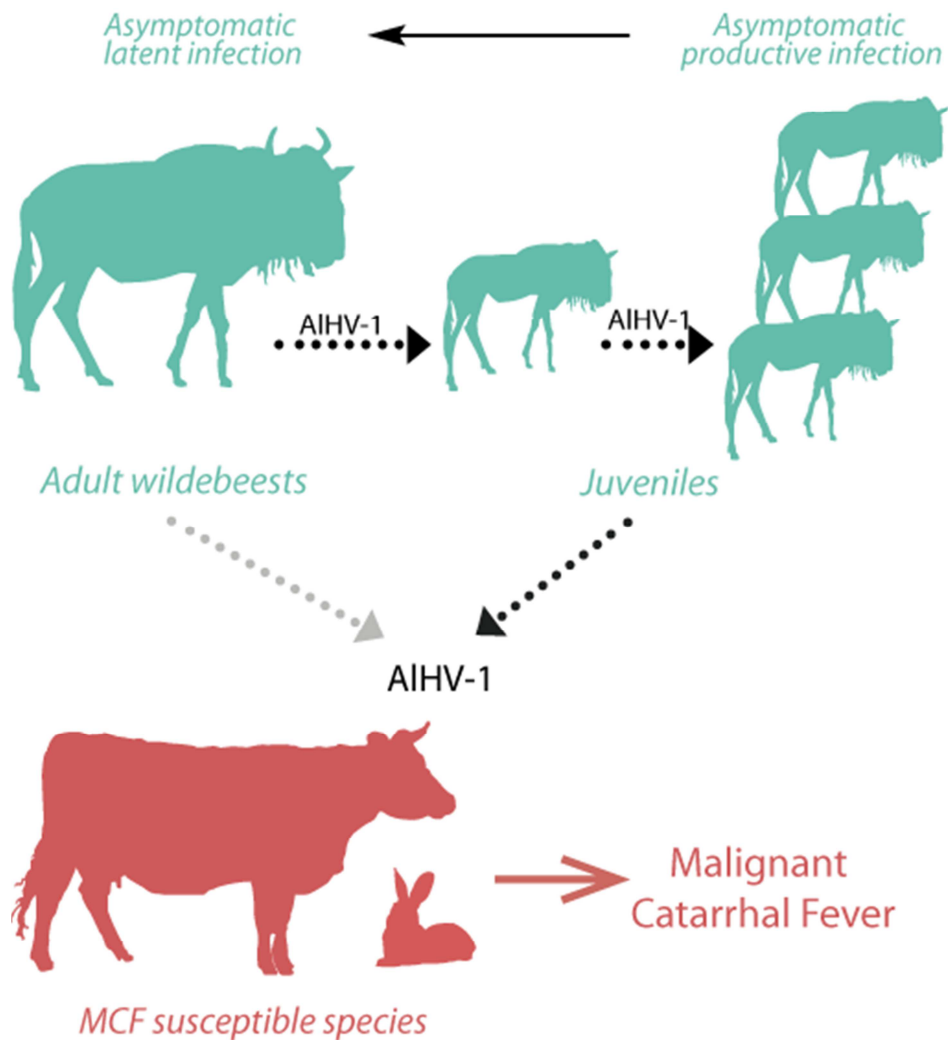


Figure 4. Natural host and alcelaphine herpesvirus 1 transmission to susceptible species. AIHV-1 infection in wildebeest is asymptomatic. During viral reactivation, wildebeest calves become infected essentially through horizontal transmission. In wildebeest calves, viral particles replicate and are excreted in nasal secretions. Young infected widebeest are infectious with a peak of infectivity around ± 4 months. Then, the latent infection is established for the rest of their life. During the period of viral excretion, AIHV-1 can be transmitted to other susceptible species such as a large number of ruminant species including cattle. After infection, susceptible species develop wildebeest-derived malignant catarrhal fever (WD-MCF). The rabbit is used as an experimental model and develop WD-MCF in a similar way as what is observed in cattle. Susceptible species represent an epidemiological dead-end meaning that they are not able to transmit the disease.

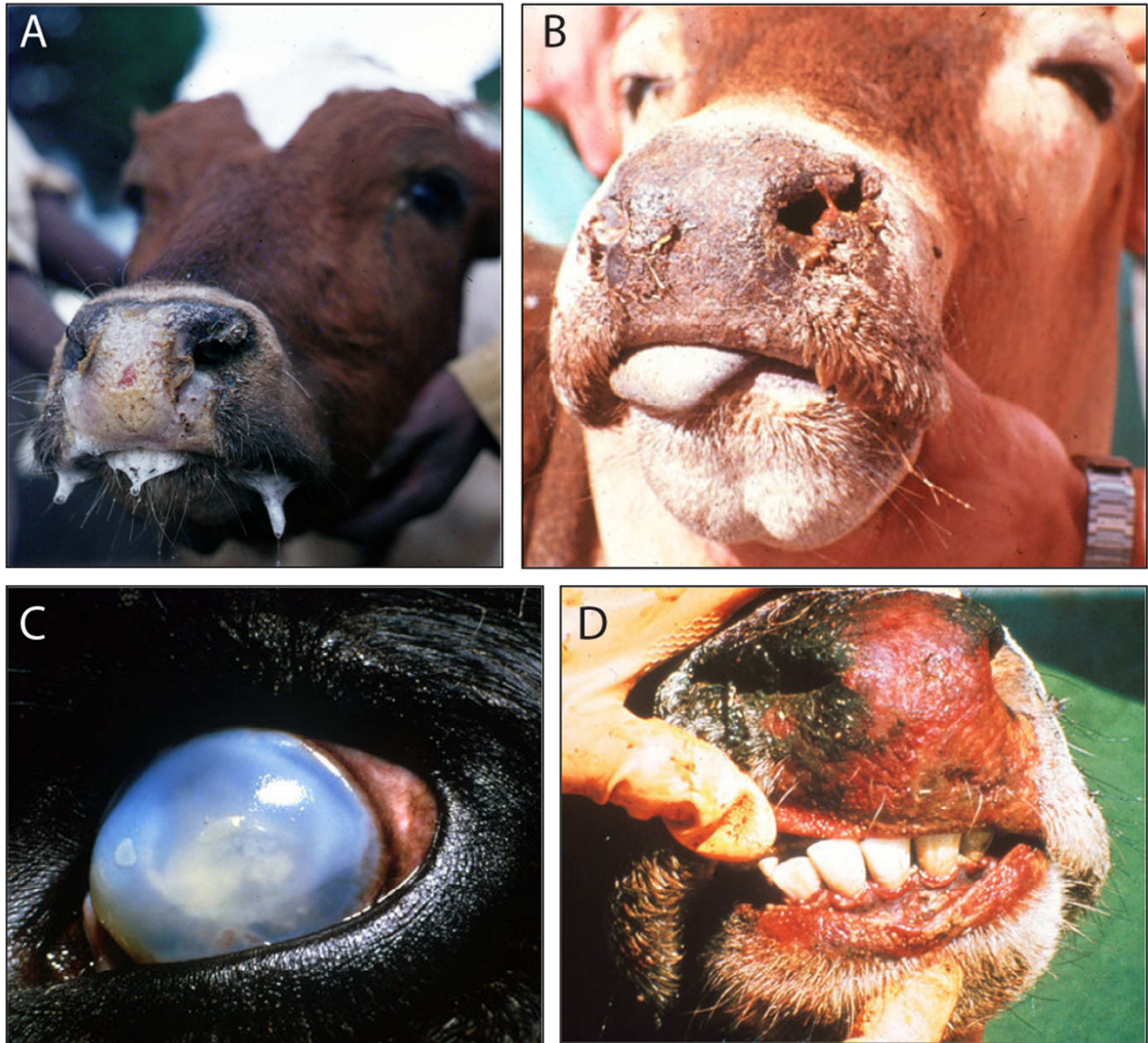


Figure 5. Typical clinical signs of wildebeest-derived malignant catarrhal fever. (A) A cow showing ptyalism, mucopurulent nasal discharge and crusting of the muzzle. **(B)** Detailed lesion of the muzzle of a cow infected with AIHV-1 showing the presence of an adherent fibrino-necrotic exudate that partially obstructs nasal cavities. **(C)** Corneal opacity in a cow developing WD-MCF. **(D)** Presence of a bright red gum line associated with an ulcerative stomatitis in a cow infected with AIHV-1. (illustrations provided by the «*Food and Agriculture Organisation of the United Nations*»).

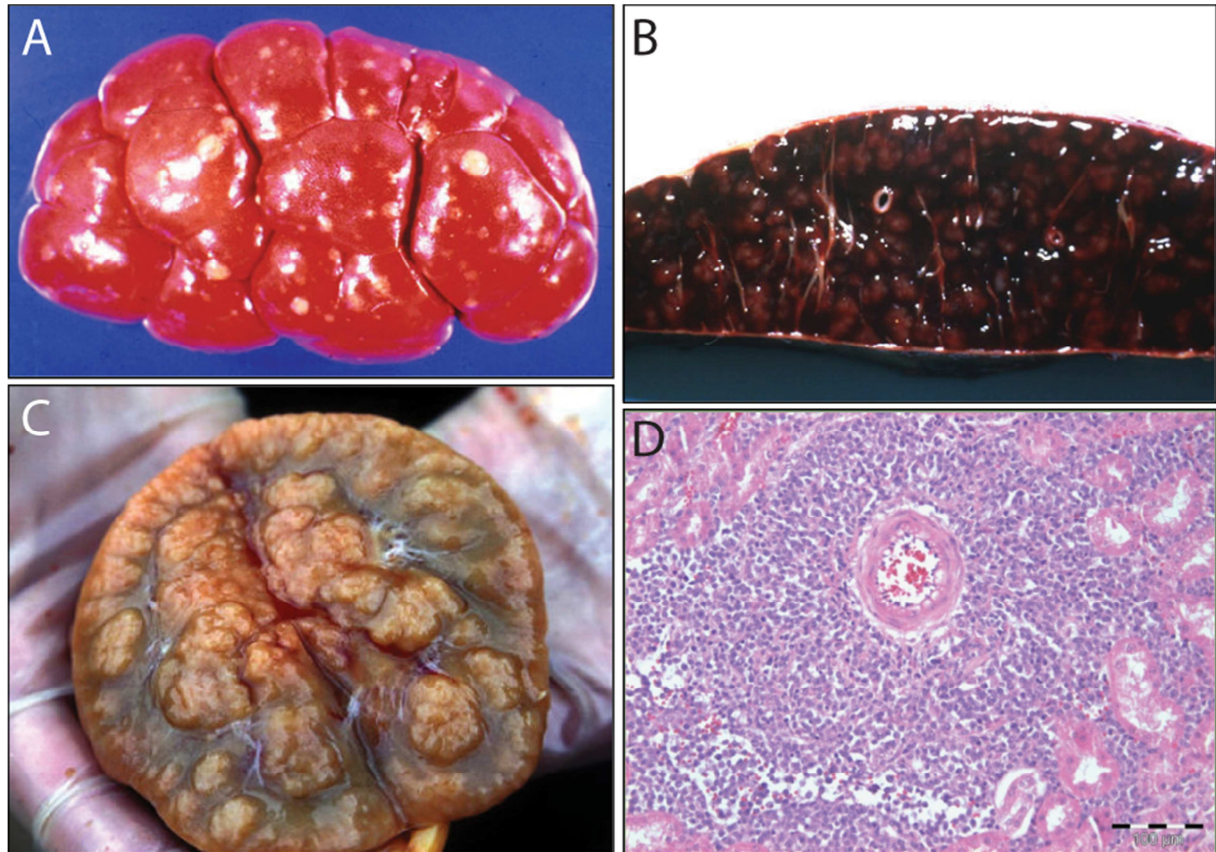


Figure 6. Lesions observed in wildebeest-derived malignant catarrhal fever-developing cattle. (A) Kidney taken from a cow infected with AIHV-1. Circumscribed white spots of a few millimeters in diameter are irregularly spread and distort the kidney surface. (B) Spleen lesions taken from a cow infected with AIHV-1. Note the heterogeneous nature of the splenic parenchyma. (C) Longitudinal section in a peripheral lymph node taken from a WD-MCF-developing cow. Note the loss of normal tissue structure in the organ and the necrotic aspect. (D) Histological section in the renal cortex of a rabbit infected with AIHV-1, stained using haematoxylin and eosin. Image was focused on a subacute per-arteriolitis lesion which is typical of WD-MCF and induced by infiltration of lymphoblastoid cells in the perivascular space. (Illustrations provided by the « Food and Agriculture Organisation of the United Nations »).

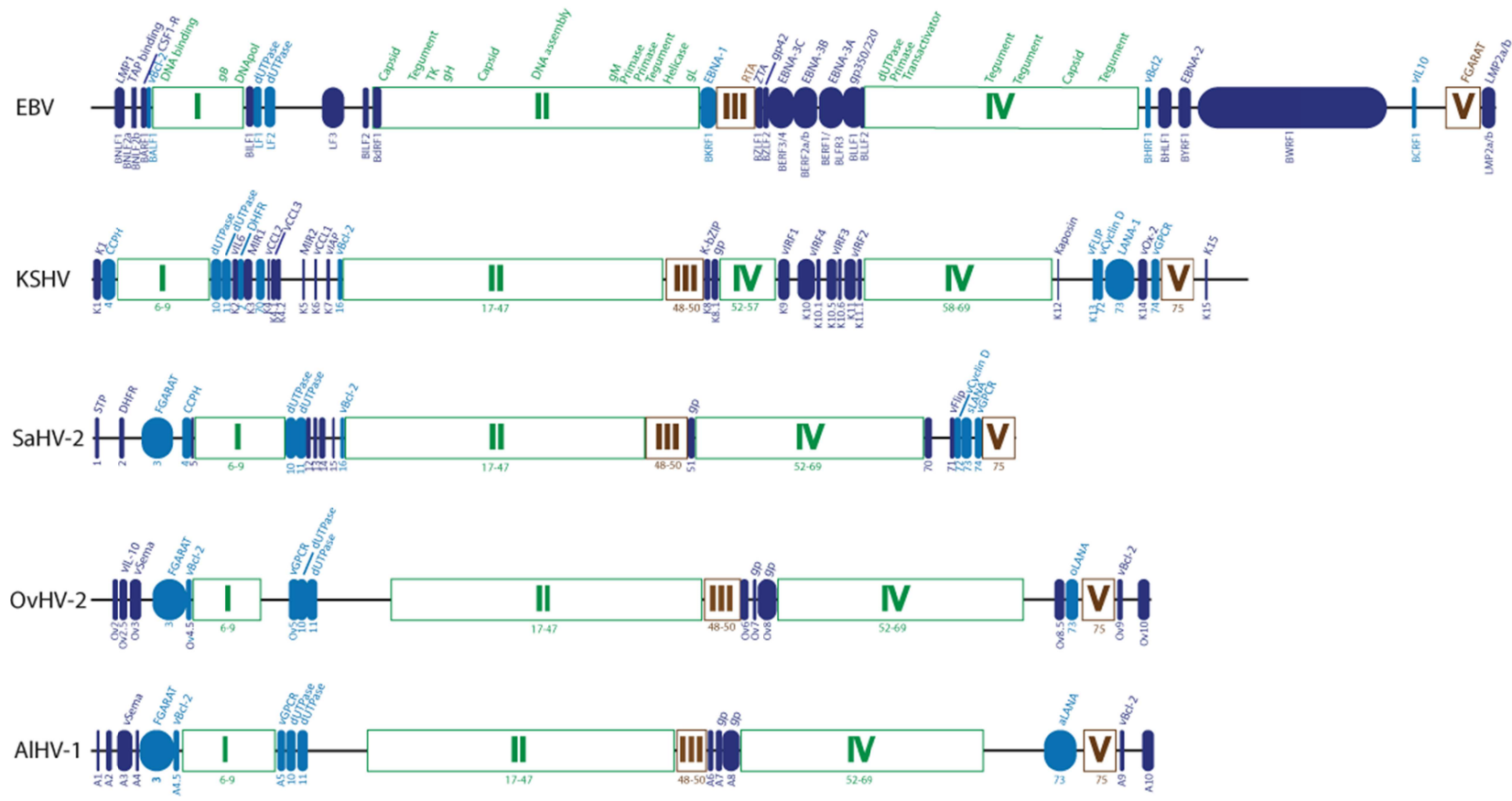


Figure 7. Genome organization of the coding region of several selected gammaherpesviruses. AIHV-1 C500 strain ([NC_002531](#)) (Ensser *et al.*, 1997) was aligned with OvHV-2 ([NC_007646](#)) (Hart *et al.*, 2007), SaHV-2 ([NC_001350](#)) (Albrecht *et al.*, 1992; Fickenscher & Fleckenstein, 2001), KSHV ([NC_009333](#)) (Rezaee *et al.*, 2006; Russo *et al.*, 1996) and EBV (de Jesus *et al.*, 2003) ([NC_007605](#)) genomes. Blocks conserved in herpesviruses are shown in green. Blocks conserved in gammaherpesviruses are depicted in brown. In variable regions, genes shared by several gammaherpesviruses are shown in light blue whereas specific genes are depicted in dark blue. ORFs are indicated below the genome illustration and corresponding proteins are shown above. Viral genes homologous to cellular genes are indicated by their abbreviation preceded by the «v» letter. DNAPol : DNA polymerase ; Bcl-2 : B-cell lymphoma 2, anti-apoptotic protein; CCL : cellular chemokine ligand ; CCPH : complement control protein homolog; CSF1-R : colony stimulating factor 1 receptor ; DHFR : dihydrofolate reductase ; EBNA : Epstein-barr virus nuclear antigen ; FGARAT : phosphoribosylformylglycinamide amidotransferase; Flip : FLICE inhibitory protein, anti-apoptotic protein; gp : glycoprotein ; GPCR : G protein-coupled receptor ; IAP : inhibitor of apoptosis ; IL-6 : interleukin 6 ; IL-10 : interleukin 10 ; IRF : interferon regulatory factor ; KbZip : KSHV basic leucine zipper protein; LANA : latency-associated nuclear antigen ; LMP : latent membrane protein ; MIR : modulator of immune recognition ; GMP : genomic maintenance protein ; RTA : replication and transcription activator; Sema : semaphorin protein ; STP : SaHV-2 transforming protein ; TAP : transporter associated with antigen processing on MHC class I; TK : thymidine kinase ; ZTA : ZEBRA transcription activator.

Table II. AIHV-1 and OvHV-2 specific genes

AIHV-1 ORF	OvHV-2 ORF	% identity ^a	Protein ^b	Description ^c
A1	-	-	-	-
A2	Ov2	56	-	Contains a « leucine zipper » domain Transcription factor (Parameswaran <i>et al.</i> , 2014)
-	Ov2.5	-	vIL-10	Stimulates proliferation of mast cells Inhibits IL-8 production by macrophages (Jayawardane <i>et al.</i> , 2008)
A3	Ov3	50	Cellular Sema 7A homolog	Possible interaction with DCs functions in the natural host Dispensable for MCF induction in rabbits (Myster <i>et al.</i> , 2015)
-	Ov3.5	-	-	-
A4	-	-	-	-
A4.5	Ov4.5	50	vBcl-2	Possible anti-apoptotic role
A5	Ov5	49	vGPCR	Inhibits CREB signalling pathway Nonessential for MCF induction in rabbits (Boudry <i>et al.</i> , 2007)
A6	Ov6	28	-	Contains a « leucine zipper » domain Possible transcription factor
A7	Ov7	60	gp42 homolog (EBV)	-
A8	Ov8	41	gp350 homolog (EBV)	Multiple predicted glycosylation sites
-	Ov8.5	-	-	-
A9	Ov9	50	vBcl-2	Possible anti-apoptotic role
A9.5	Ov9.5	24	-	Secreted glycoprotein (Russell <i>et al.</i> , 2013)
A10	Ov10	22	-	Contains a nuclear localization signal

^aThe percentage of amino-acid sequence identity was calculated with blastp. Percent identity between conserved genes of AIHV-1 and OvHV-2 has been shown to vary between 36 and 83 % (Hart *et al.*, 2007).

^bIdentification based on sequence homology or positional homology. IL-10 : interleukin 10 ; Sema7A: semaphorin 7A ; DCs : dendritic cells ; Bcl-2 : B-cell lymphoma 2, anti-apoptotic protein ; GPCR : G protein-coupled receptor ; gp : glycoprotein ; gp42 and gp350 : EBV glycoproteins involved in virus entry.

^cRoles based on analysis of predicted amino-acid sequences (except for A2, A3, A5, A9.5 and Ov2.5). IL-8 : interleukin 8.

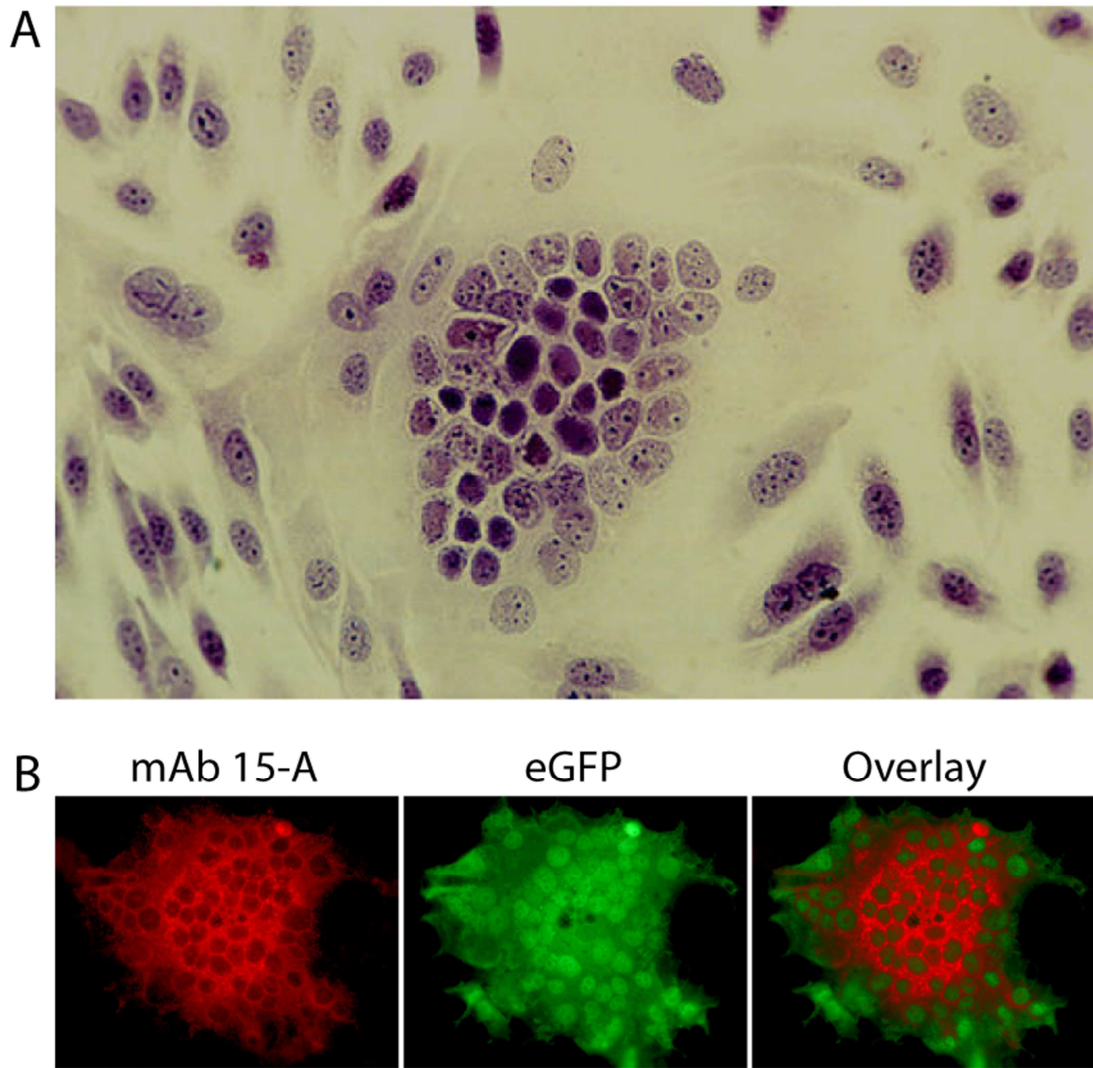


Figure 8. *In vitro* cytopathogenic effect induced by AIHV-1 infection in cell culture. (A) In the center, giant multinucleated cell (*syncytium*), typical of the cytopathogenic effect during AIHV-1 infection of cells of bovine origin. (illustration conducted by P.B. Rossiter et provided by the « *Food and Agriculture Organisation of the United Nations* »). (B) Madin-Darby bovine kidney cells infected with AIHV-1 BAC (Dewals *et al.*, 2006). Cells were stained with an antibody specific to 15-A epitope (mAb 15-A) from the gp115 glycoprotein complex of AIHV-1 (Li *et al.*, 1995). This was followed by secondary staining with Alexa Fluor 568nm-conjugated goat anti-mouse IgG polyserum. EGFP is expressed in syncytia because of the presence of the eGFP expression cassette in AIHV-1 BAC.

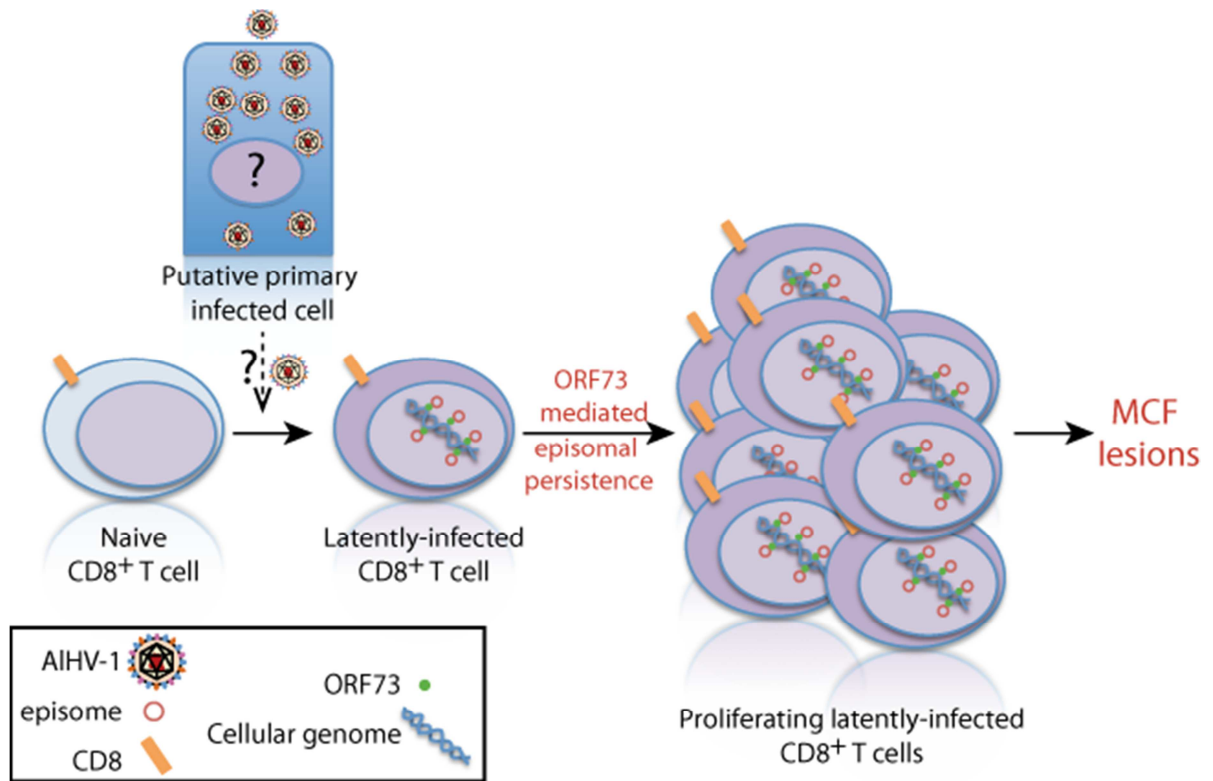


Figure 9. Proposed model for the pathogenesis of malignant catarrhal fever. After a putative primary productive infection in unknown cell subtypes, CD8⁺ T cells are infected by AIHV-1. The virus remains latent, and viral episomes are maintained in the nucleus of infected cells through expression of ORF73. Subsequently, virus-induced cell proliferation ultimately occurs, leading to the typical perivascular infiltrates in most tissues.

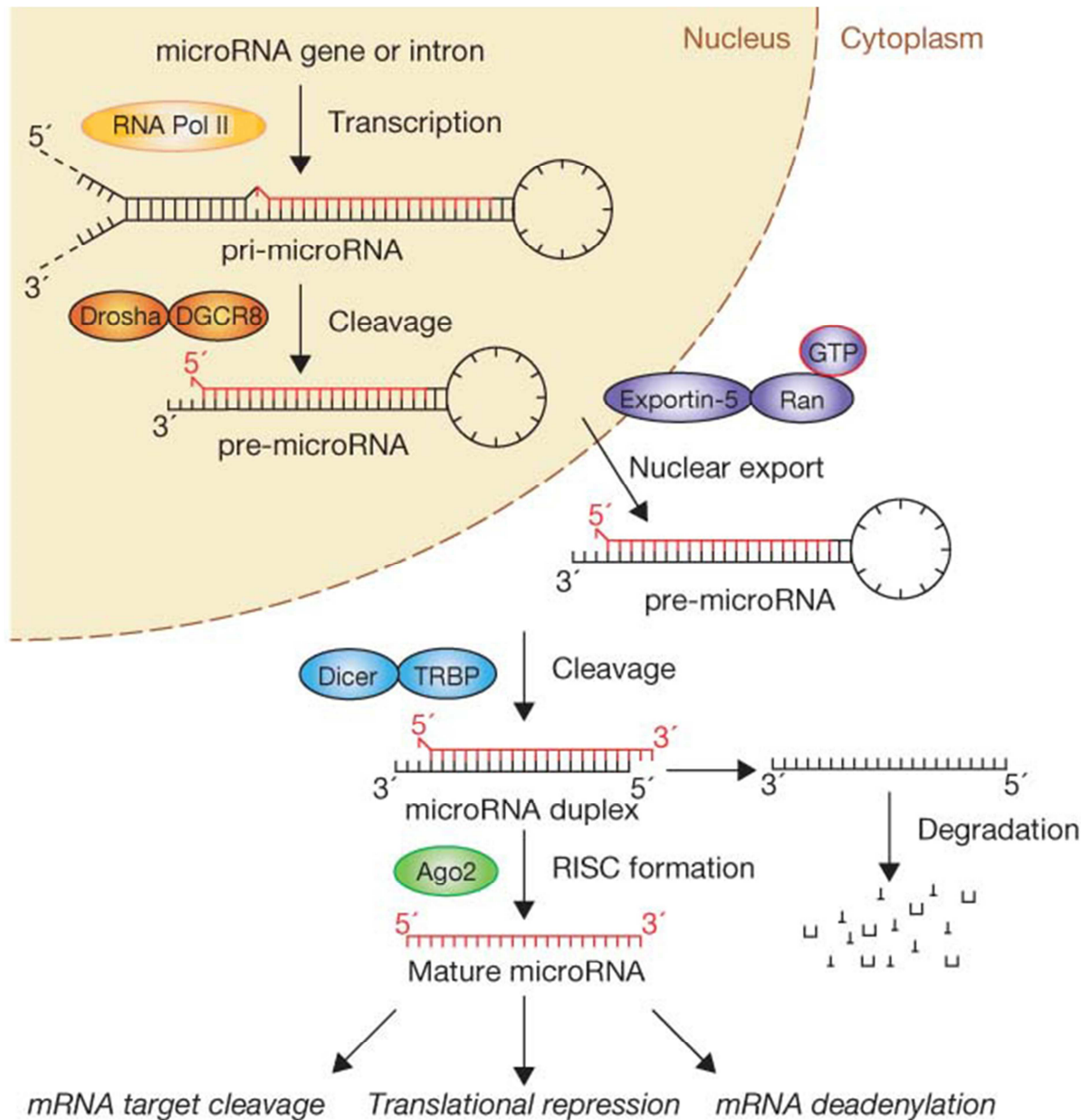


Figure 10. Canonical miRNA biogenesis. This canonical maturation includes the production of the primary miRNA transcript (pri-miRNA) by RNA polymerase II and cleavage of the pri-miRNA by the microprocessor complex Drosha-DGCR8 in the nucleus. The resulting precursor hairpin, the pre-miRNA, is exported from the nucleus by Exportin-5-Ran-GTP. In the cytoplasm, the RNase Dicer in complex with the double-stranded RNA-binding protein TRBP cleaves the pre-miRNA hairpin to its mature length. The functional strand of the mature miRNA is loaded together with Argonaute (Ago2) proteins into the RNA-induced silencing complex (RISC), where it guides RISC to silence target mRNAs through mRNA cleavage, translational repression or deadenylation, whereas the passenger strand (shown in black) is degraded. Adapted from Winter *et al.* (2009).

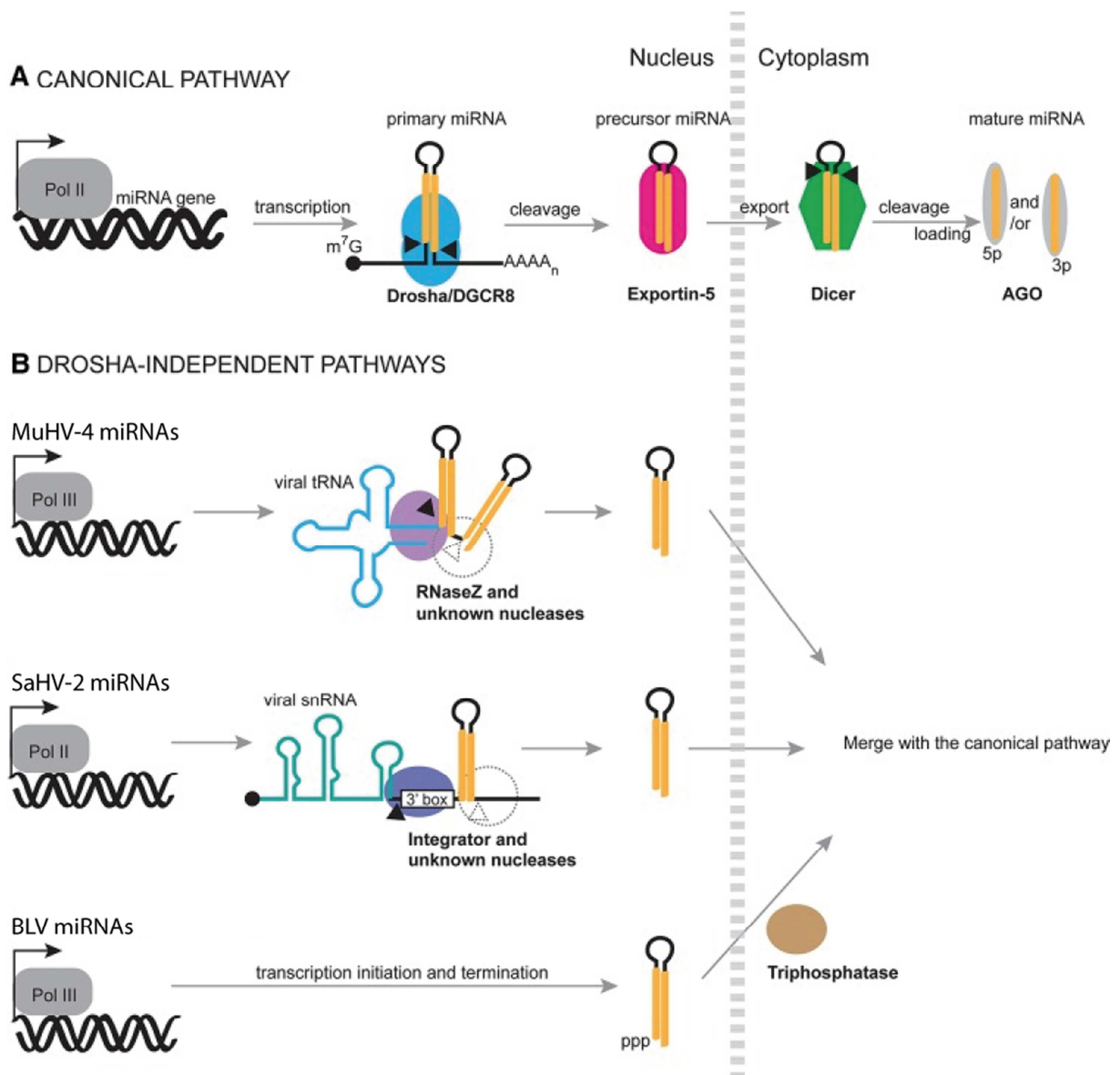


Figure 11. Canonical and non-canonical pathways of miRNA biogenesis. (A) The canonical pathway. pri-miRNAs are typically transcribed by RNA Pol II, 5'-capped, and 3'-polyadenylated. The Microprocessor complex (Drosha and DGCR8) cleaves pri-miRNAs to release pre-miRNA hairpins, which are exported by Exportin-5 and processed by Dicer into mature miRNA duplexes in the cytoplasm. One miRNA strand is preferentially selected by AGO to form RISCs. (B) Drosha-independent miRNA biogenesis in animal viruses. *Murid herpesvirus 4* (MuHV-4) pri-miRNAs are tRNA-pre-miRNA chimeras that are processed by RNaseZ at the 5' end of the first pre-miRNA hairpin. The enzyme that separates the two pre-miRNAs is unknown. *Saimiriine herpesvirus 2* (SaHV-2) pri-miRNAs are snRNA-pre-miRNA chimeras that are processed by Integrator to release the pre-miRNA. The 3' end formation mechanism for SaHV-2 pre-miRNAs remains elusive. *Bovine leukemia virus* (BLV) miRNAs are derived from pre-miRNAs that are directly transcribed by RNA Pol III as endogenous shRNAs. All viral pre-miRNAs pictured are exported by XPO5 and processed by Dicer. Adapted from Tycowski *et al.* (2015).

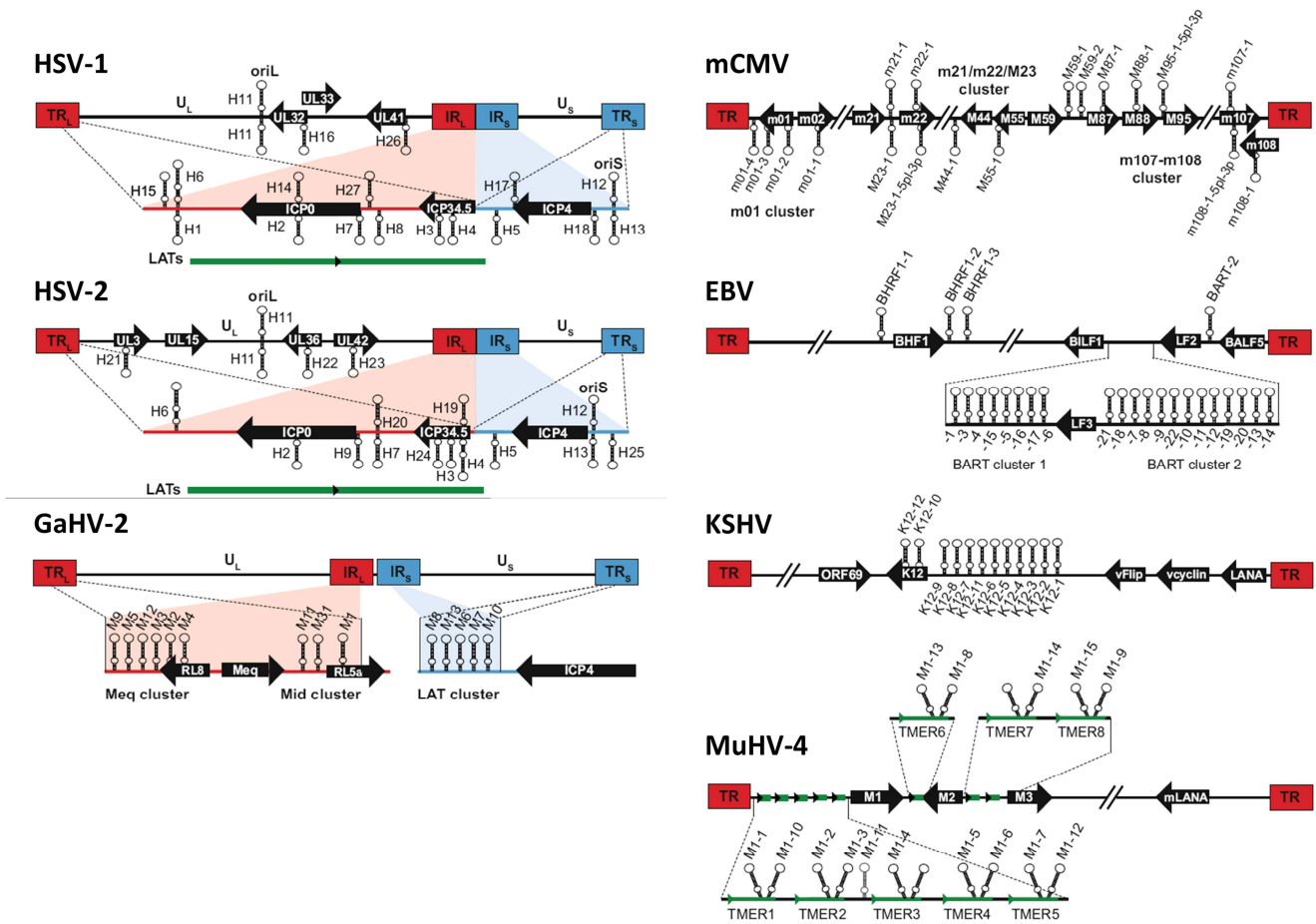


Figure 12. Genomic location of herpesvirus pre-miRNAs. Genomic maps indicate the number of miRNA stem-loops and approximate locations of miRNAs relative to one another and to nearby transcripts. Pre-miRNA stem-loops depicted above genomes are encoded by the forward strand and those depicted below genomes are encoded by the reverse strand. Nearby coding genes are represented by black arrows, and adjacent non-coding transcripts are represented by green lines. HSV-1, HSV-2 and GaHV-2 encode miRNA precursors within both the internal (IR) and terminal (TR) repeats, as indicated. Depictions of genomes and transcripts are not to scale. U_s, unique short; U_L, unique long; LAT, latency associated transcript; TMER, t-RNA-microRNA encoded RNA. Adapted from Feldman and Tibbetts (2015).

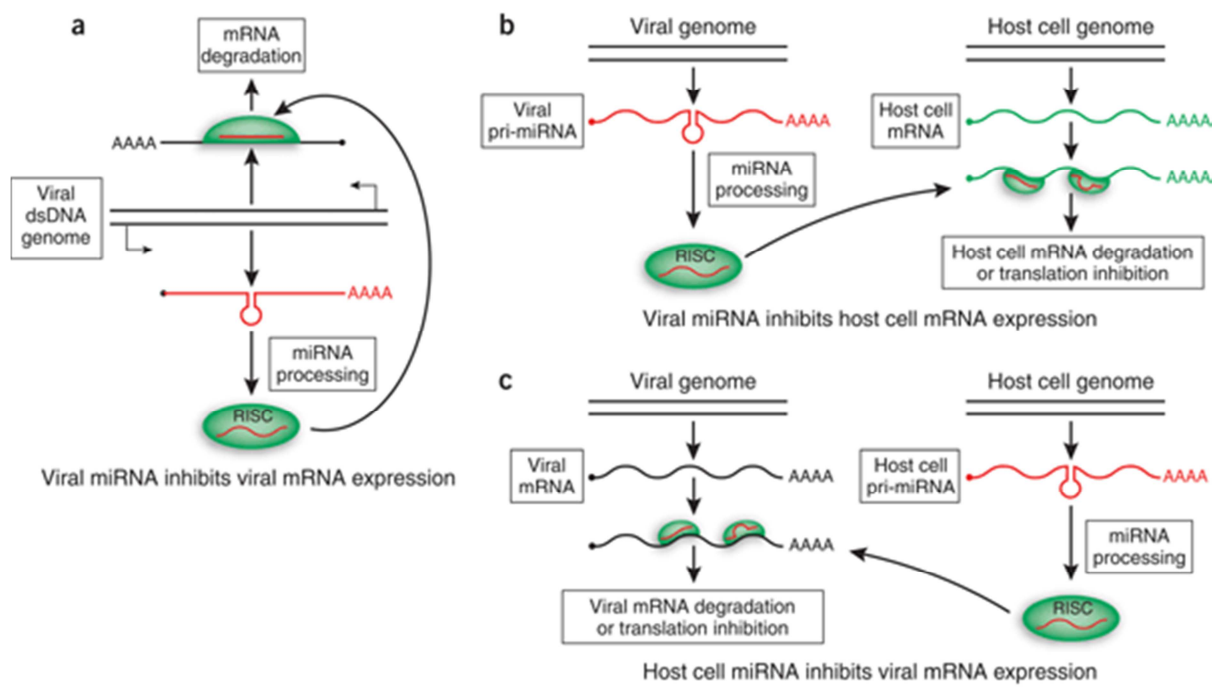
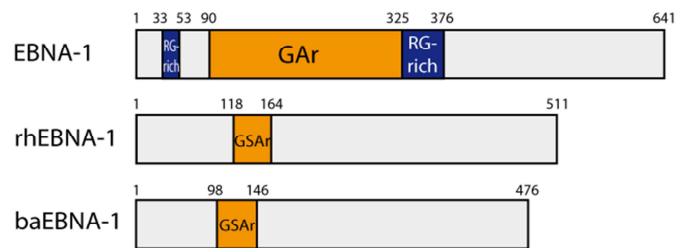


Figure 13. Potential mechanisms by which miRNAs can affect virus replication. (a) Viral miRNAs may inhibit the expression of viral mRNAs. As shown, these are perfectly complementary mRNAs that are transcribed from the strand of a viral DNA genome that lies opposite the miRNA gene, but inhibition of mRNAs transcribed from other regions of the viral genome is possible. dsDNA, double-stranded DNA. (b) Viral miRNAs may also inhibit the expression of cellular mRNAs. (c) Finally, cellular miRNAs could inhibit the expression of viral mRNAs. Adapted from Cullen (2006).

Lymphocryptovirus GMPs



Rhadinovirus GMPs

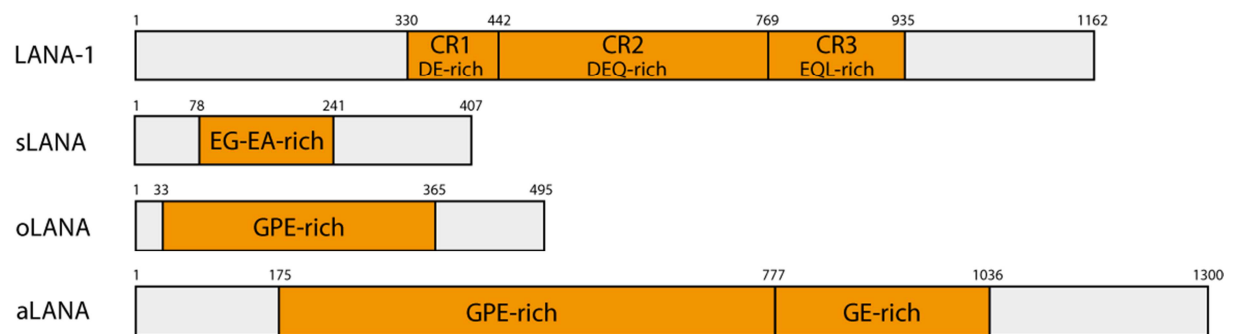


Figure 14. Schematic representation of several gammaherpesvirus GMPs. N- and C-terminal domains are separated by various-sized central amino acid repeat domains, highlighted in orange, containing the indicated amino acids. The RG-rich regions of EBNA-1 are depicted in blue. Lymphocryptoviruses : EBNA-1 (EBV, B95.8 strain), rhEBNA1 (rhLCV, LCL8664 strain) and baEBNA-1 (baLCV, S594 strain). Rhadinoviruses: LANA-1 (KSHV, BC-1 strain), sLANA (SaHV-2, A11 strain), oLANA (OvHV-2, BJ035 strain) and aLANA (AIHV-1, C500 strain).

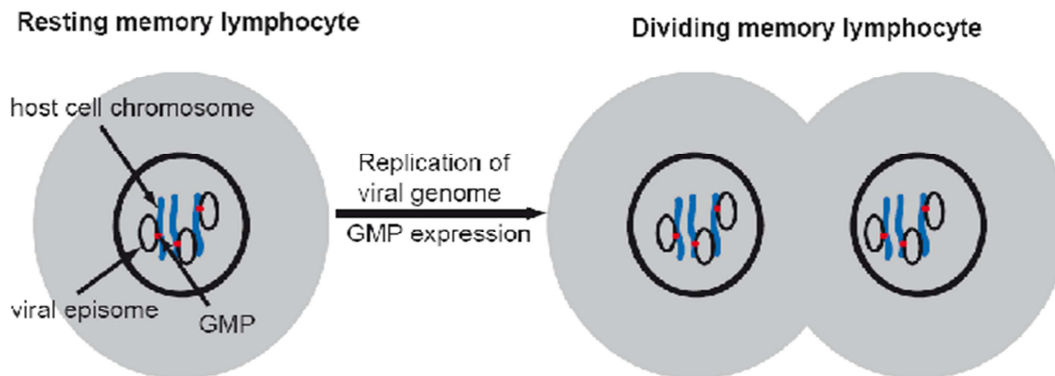


Figure 15. Model for the role of GMPs that allows gammaherpesviruses to maintain a latent infection of their host. From Blake (2010).

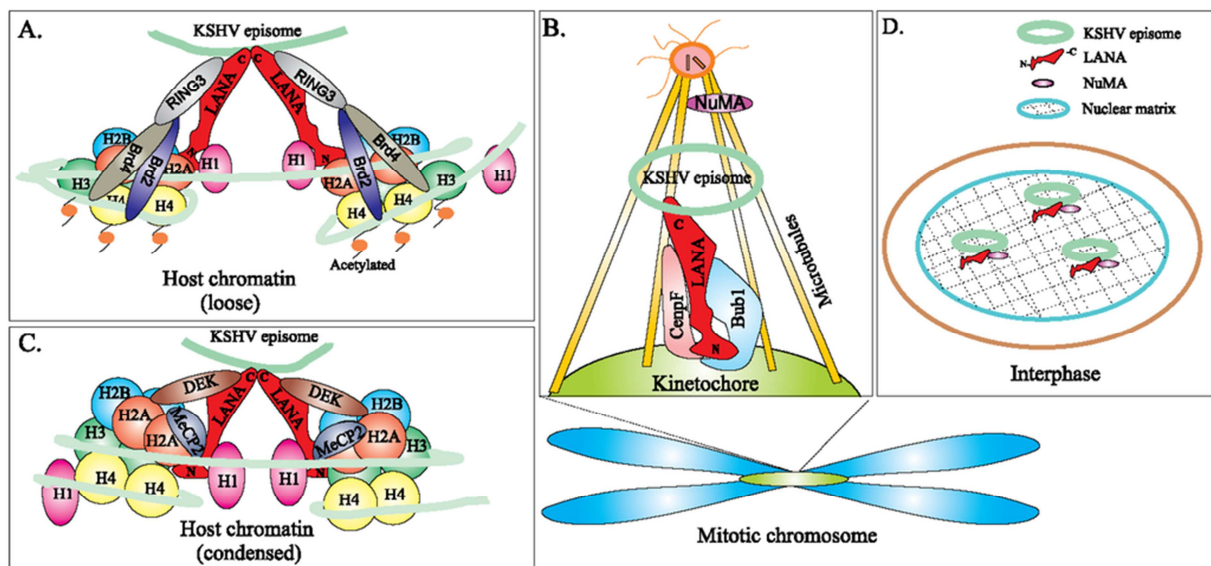


Figure 16. Schematic model showing the association of KSHV LANA with host proteins that aid in tethering to the host chromatin and segregation. The interaction of host cellular proteins with LANA during interphase (panel D) and the Mitotic phase (M-phase) is shown. During interphase, NuMA binds to the nuclear matrix and tethers KSHV genome by interacting with the carboxy-terminus of LANA, whereas during the M-phase, this interaction is lost and NuMA interacts with the microtubules and localizes to the spindle poles. Panel A shows a loose chromatin structure, where the host chromatin-binding protein BRD2/RING3 interacts with acetylated histone H4 and BRD4 interacts with acetylated histones H3 and H4, whereas LANA binds to the RING3 through the C-terminal domain, thus showing the contribution of host BET proteins in KSHV genome persistence. Panel B shows that both the N- and C-terminus of LANA strongly bind to the kinetochore proteins Bub1 and CENP-F that ensures delivery of KSHV episomes to the daughter cells during chromatid segregation. Panel C shows the condensed chromatin structure during M-phase. LANA interacts with the core histone proteins (H2A, H2B, H3 and H4) through the N-terminal domain and binds to the KSHV episome through the C-terminal domain. Nucleosome binding by the chromatin-binding motif facilitates interaction of LANA with MeCP2 at the N-terminal domain of LANA. DEK protein interacts with the C-terminal domain of LANA and also to histones H2A, H2B, H3 and H4 facilitating tethering of LANA to the host chromatin. Adapted from Uppal *et al.* (2014).

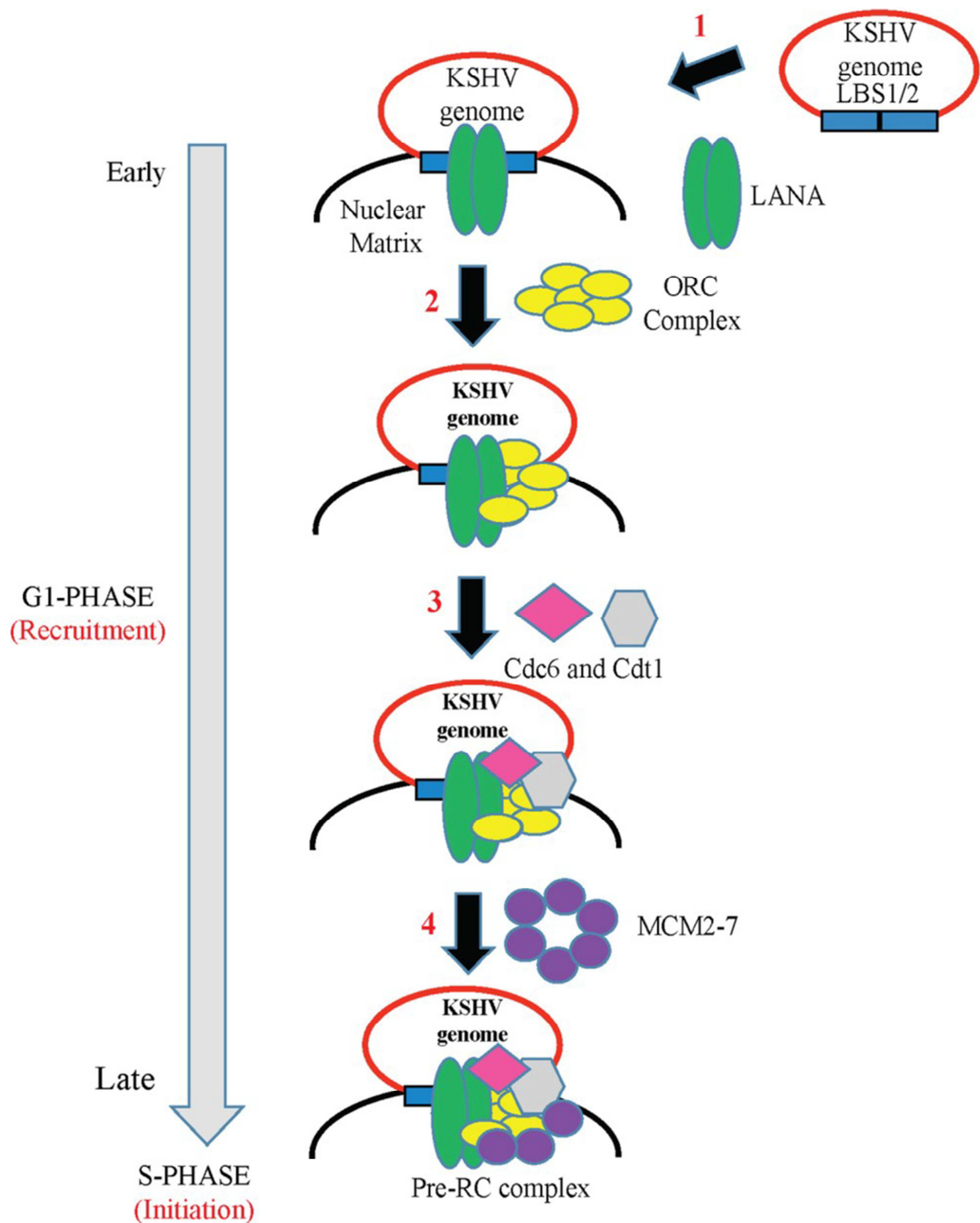


Figure 17. A model of the KSHV latent DNA replication. (1) LANA binds to the LANA-binding sites (LBS1 and LBS2) or replication origin of the terminal repeats (TR) region of the KSHV genome and recruits it to the nuclear matrix region; (2) LANA then recruits the host cellular machinery factors such as Origin Replication Complexes (ORCs) to the replication origin which is followed by (3) sequential loading of Cdc6, Cdt1; and (4) heterohexameric complex Mcm2-7 to the origins to form pre-replicative complex (pre-RC) during late G1 phase followed by replication of DNA during early S phase. From Uppal *et al.* (2014).

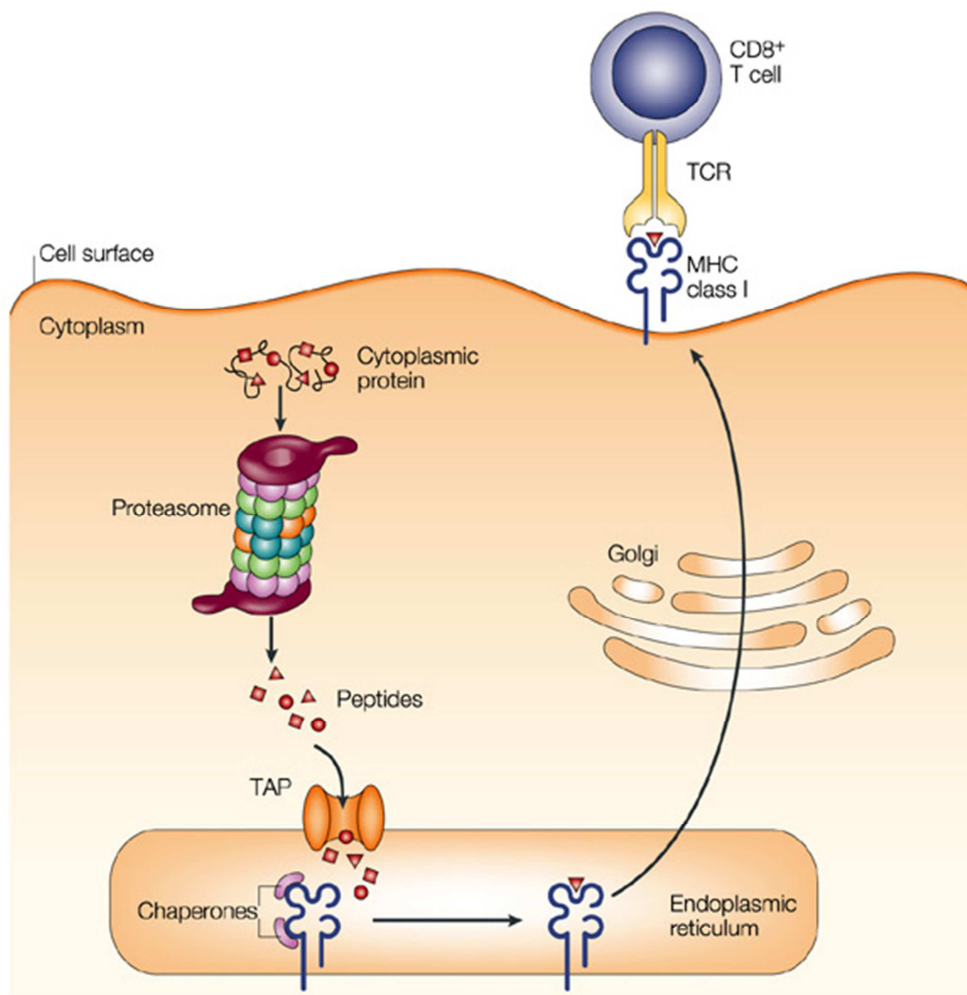


Figure 18. The MHC class I antigen presentation pathway. Cytosolic and nuclear proteins are degraded by the proteasome into peptides. The transporter for antigen processing (TAP) then translocates peptides into the lumen of the endoplasmic reticulum (ER) while consuming ATP. MHC class I heterodimers wait in the ER for the third subunit, a peptide. Peptide binding is required for correct folding of MHC class I molecules and release from the ER and transport to the plasma membrane, where the peptide is presented to the immune system. TCR, T-cell receptor. Adapted from Yewdell *et al.* (2003).

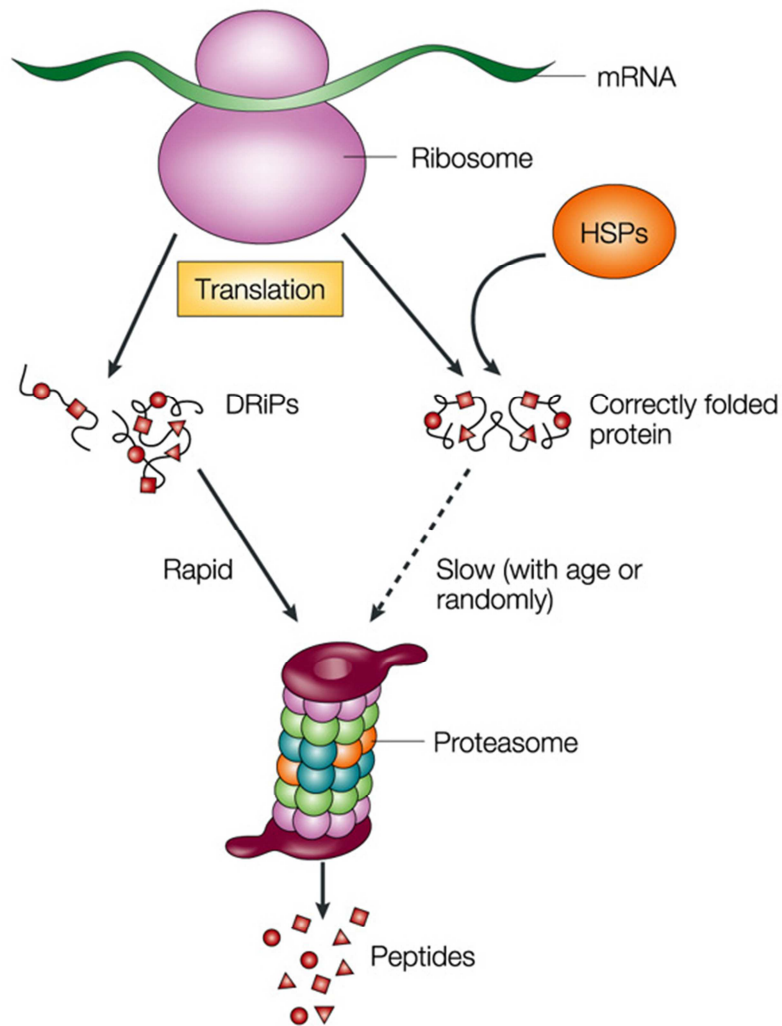


Figure 19. The DRiPs hypothesis. All proteins are made by ribosomes using messenger RNA as a template. Nascent proteins are frequently stabilized by heat-shock proteins (HSPs), which probably facilitate folding by preventing aggregation. Despite this, a marked fraction of translation products is defective, resulting in incorrect (mistranslated or prematurely stopped), misfolded or misassembled proteins. These defective ribosomal products (DRiPs) are shunted to the proteasome for degradation, coupling protein production to MHC class I antigen presentation, and enable a rapid T-cell response to new viral proteins. Adapted from Yewdell *et al.* (2003).

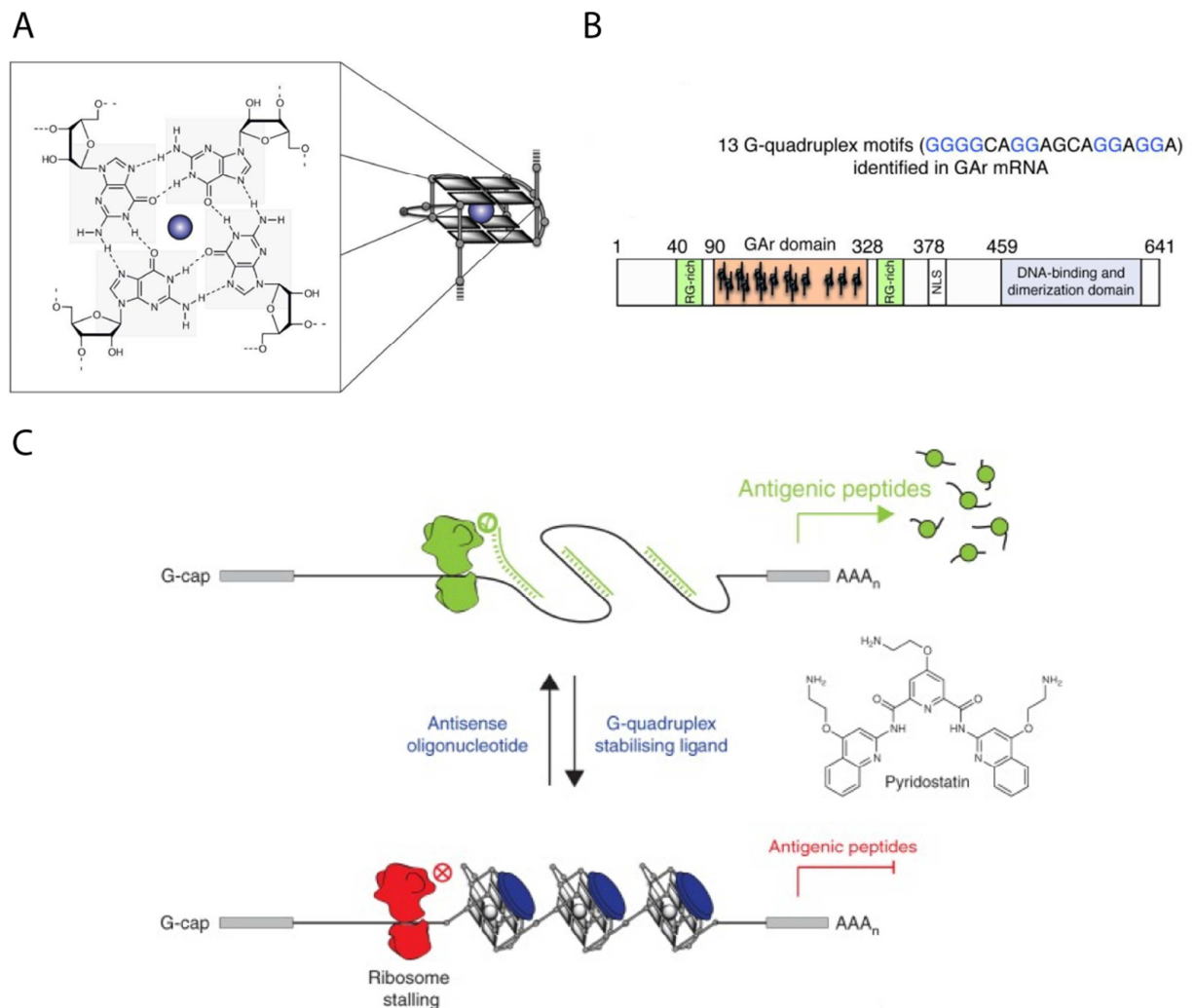


Figure 20. Identification and characterization of G-quadruplex structures within the EBNA-1 GAR mRNA. (A) A guanine tetrad formed by the coplanar arrangement of four guanine bases held together by Hoogsteen hydrogen bonds and stabilized by a cation (usually potassium, depicted in blue) to constitute a G-quadruplex structure. (B) Schematic representation of EBV EBNA-1 depicting the domains essential for genome maintenance functions. Highlighted within the internal GAR domain are the positions of G4-EBNA-1 G-quadruplex motifs identified in the corresponding mRNA. The G4-EBNA-1 schematic depicts an EBNA-1 intramolecular parallel G-quadruplex stabilized by the stacking of two guanine tetrads (gray squares represent guanines as depicted in (A)). (C) Destabilization or stabilization of G-quadruplexes using antisense oligonucleotides or small molecule G-quadruplex ligands (Pyridostatin), respectively, stimulates or inhibits the synthesis of the EBV-genome maintenance protein, EBNA-1, and subsequent generation and presentation of MHC class I restricted antigenic peptides. Adapted from Murat *et al.* (2014) and Murat and Tellam (2015).

- Albrecht, J. C., Nicholas, J., Biller, D., Cameron, K. R., Biesinger, B., Newman, C., Wittmann, S., Craxton, M. A., Coleman, H., Fleckenstein, B. & et al. (1992).** Primary structure of the herpesvirus saimiri genome. *J Virol* **66**, 5047-5058.
- Blake, N. (2010).** Immune evasion by gammaherpesvirus genome maintenance proteins. *J Gen Virol* **91**, 829-846.
- Boudry, C., Markine-Goriaynoff, N., Delforge, C., Springael, J. Y., de Leval, L., Drion, P., Russell, G., Haig, D. M., Vanderplasschen, A. F. & Dewals, B. (2007).** The A5 gene of alcelaphine herpesvirus 1 encodes a constitutively active G-protein-coupled receptor that is non-essential for the induction of malignant catarrhal fever in rabbits. *J Gen Virol* **88**, 3224-3233.
- Davison, A. J. (2011).** Evolution of sexually transmitted and sexually transmissible human herpesviruses. *Ann N Y Acad Sci* **1230**, E37-49.
- de Jesus, O., Smith, P. R., Spender, L. C., Elgueta Karstegl, C., Niller, H. H., Huang, D. & Farrell, P. J. (2003).** Updated Epstein-Barr virus (EBV) DNA sequence and analysis of a promoter for the BART (CST, BARF0) RNAs of EBV. *J Gen Virol* **84**, 1443-1450.
- Dewals, B., Boudry, C., Gillet, L., Markine-Goriaynoff, N., de Leval, L., Haig, D. M. & Vanderplasschen, A. (2006).** Cloning of the genome of Alcelaphine herpesvirus 1 as an infectious and pathogenic bacterial artificial chromosome. *J Gen Virol* **87**, 509-517.
- Enquist, L. W., Krug, R. M., Racaniello, V. R., A.M., S. & Flint, S. J. (2000).** *Principles of Virology: Molecular Biology, Pathogenesis, and Control*. Washington D.C.
- Ensser, A., Pflanz, R. & Fleckenstein, B. (1997).** Primary structure of the alcelaphine herpesvirus 1 genome. *J Virol* **71**, 6517-6525.
- Feldman, E. R. & Tibbetts, S. A. (2015).** Emerging Roles of Herpesvirus microRNAs During In Vivo Infection and Pathogenesis. *Current pathobiology reports* **3**, 209-217.
- Fickenscher, H. & Fleckenstein, B. (2001).** Herpesvirus saimiri. *Philos Trans R Soc Lond B Biol Sci* **356**, 545-567.
- Hart, J., Ackermann, M., Jayawardane, G., Russell, G., Haig, D. M., Reid, H. & Stewart, J. P. (2007).** Complete sequence and analysis of the ovine herpesvirus 2 genome. *J Gen Virol* **88**, 28-39.
- Jayawardane, G., Russell, G. C., Thomson, J., Deane, D., Cox, H., Gatherer, D., Ackermann, M., Haig, D. M. & Stewart, J. P. (2008).** A captured viral interleukin 10 gene with cellular exon structure. *J Gen Virol* **89**, 2447-2455.
- Li, H., Shen, D. T., Davis, W. C., Knowles, D. P., Gorham, J. R. & Crawford, T. B. (1995).** Identification and characterization of the major proteins of malignant catarrhal fever virus. *J Gen Virol* **76** (Pt 1), 123-129.
- Murat, P. & Tellam, J. (2015).** Effects of messenger RNA structure and other translational control mechanisms on major histocompatibility complex-I mediated antigen presentation. *Wiley interdisciplinary reviews RNA* **6**, 157-171.

- Murat, P., Zhong, J., Lekieffre, L., Cowieson, N. P., Clancy, J. L., Preiss, T., Balasubramanian, S., Khanna, R. & Tellam, J. (2014).** G-quadruplexes regulate Epstein-Barr virus-encoded nuclear antigen 1 mRNA translation. *Nat Chem Biol* **10**, 358-364.
- Myster, F., Palmeira, L., Sorel, O., Bouillenne, F., DePauw, E., Schwartz-Cornil, I., Vanderplasschen, A. & Dewals, B. G. (2015).** Viral semaphorin inhibits dendritic cell phagocytosis and migration but is not essential for gammaherpesvirus-induced lymphoproliferation in malignant catarrhal fever. *J Virol* **89**, 3630-3647.
- Parameswaran, N., Dewals, B. G., Giles, T. C., Deppmann, C., Blythe, M., Vanderplasschen, A., Emes, R. D. & Haig, D. (2014).** The A2 gene of alcelaphine herpesvirus-1 is a transcriptional regulator affecting cytotoxicity in virus-infected T cells but is not required for malignant catarrhal fever induction in rabbits. *Virus Res* **188**, 68-80.
- Rezaee, S. A., Cunningham, C., Davison, A. J. & Blackbourn, D. J. (2006).** Kaposi's sarcoma-associated herpesvirus immune modulation: an overview. *J Gen Virol* **87**, 1781-1804.
- Russell, G. C., Todd, H., Deane, D., Percival, A., Dagleish, M. P., Haig, D. M. & Stewart, J. P. (2013).** A novel spliced gene in alcelaphine herpesvirus 1 encodes a glycoprotein which is secreted in vitro. *J Gen Virol* **94**, 2515-2523.
- Russo, J. J., Bohenzky, R. A., Chien, M. C., Chen, J., Yan, M., Maddalena, D., Parry, J. P., Peruzzi, D., Edelman, I. S., Chang, Y. & Moore, P. S. (1996).** Nucleotide sequence of the Kaposi sarcoma-associated herpesvirus (HHV8). *Proc Natl Acad Sci U S A* **93**, 14862-14867.
- Tycowski, K. T., Guo, Y. E., Lee, N., Moss, W. N., Vallery, T. K., Xie, M. & Steitz, J. A. (2015).** Viral noncoding RNAs: more surprises. *Genes Dev* **29**, 567-584.
- Uppal, T., Banerjee, S., Sun, Z., Verma, S. C. & Robertson, E. S. (2014).** KSHV LANA--the master regulator of KSHV latency. *Viruses* **6**, 4961-4998.
- Winter, J., Jung, S., Keller, S., Gregory, R. I. & Diederichs, S. (2009).** Many roads to maturity: microRNA biogenesis pathways and their regulation. *Nat Cell Biol* **11**, 228-234.
- Yewdell, J. W., Reits, E. & Neefjes, J. (2003).** Making sense of mass destruction: quantitating MHC class I antigen presentation. *Nat Rev Immunol* **3**, 952-961.